EXPERIMENTAL RESEARCH ON 4-DUCT TANDEM VTOL AIRCRAFT CONFIGURATIONS

M. O. McKinney and W. A. Newsom

NASA Langley Research Center
Langley Station, Hampton, Va.

Presented to the Eighteenth Annual Forum of the
American Helicopter Society

Washington, D.C.
May 3-5, 1962

EXPERIMENTAL RESEARCH ON 4-DUCT TANDEM VTOL AIRCRAFT CONFIGURATIONS

M. O. McKinney and W. A. Newsom
Aerospace Technologist
NASA Langley Research Center
Langley Station, Hampton, Va.

Summary

This paper presents a brief summary of several wind-tunnel investigations conducted at the Langley Research Center of the NASA to study the aerodynamic and stability and control characteristics of several VTOL aircraft configurations powered by four tilting ducted propellers arranged in tandem pairs. Specifically the two rear ducts could be mounted close alongside the upper rear portion of the fuselage with small wing panels attached to the outboard side of the ducts or could be mounted outboard on the tips of a small wing located high on the rear portion of the fuselage. The two front ducts were always mounted close inboard on the forward part of the fuselage and could be mounted either in a high or low position on the fuselage.

The results of the investigation indicated that aircraft of this type could have acceptable aerodynamic and static longitudinal and lateral stability and control characteristics in both transition and normal cruise flight except for the possible qualification that the lateral force due to sideslip is abnormally high and might cause the aircraft to be too sensitive to side gusts.

Introduction

For VTOL aircraft, configurations powered by four ducted propellers arranged in pairs fore and aft, as illustrated in figures 1 and 2, have certain attractive features for the VTOL phase of operation. Specifically, the tandem arrangement has certain advantages in control system simplicity for hovering and transition flight in that it is possible to achieve a large amount of pitch control efficiently by simply varying the pitch of the forward and rearward propellers. The configuration, particularly in the form shown in figure 1, also offers advantages for carrier operation in terms of compactness and ease of folding. In order to properly evaluate such novel configurations it is necessary to know something of their aerodynamic and stability and control characteristics. An exploratory series of wind-tunnel investigations has therefore been conducted at the Langley Research Center of the NASA to provide some basic aerodynamic and stability and control data on 4-duct tandem VTOL aircraft configurations. The investigation has not been completed, and the data presented herein are of a preliminary nature.

Symbols

The model configurations are designated in terms of the position of the rear ducts (inboard or outboard) and the position of the front ducts (high or low) by the following nomenclature:

IB-HI Rear ducts inboard, front ducts high

IB-LO Rear ducts inboard, front ducts low

OB-HI Rear ducts outboard, front ducts high

OB-LO Rear ducts outboard, front ducts low

These configurations are illustrated in the sketches of figures 1 and 2.

All forces and moments are referred to the stability system of axes, and the moments are also referred to a moment reference center at a station halfway between the forward and rearward duct pivot axes and halfway between the top and bottom surfaces of the fuselage.

C_L lift coefficient, $\left(\frac{L}{qS}\right)$

C_D drag coefficient, $\left(\frac{D}{qS}\right)$

C_M pitching-moment coefficient, $\left(\frac{M}{qSc}\right)$

L lift, lb

D drag, lb

M pitching moment, ft-lb

q dynamic pressure $\left(\frac{\rho V^2}{2}\right)$, lb/ft^2

V free-stream velocity

α angle of attack of fuselage centerline, deg

β angle of sideslip, deg

T_c' thrust coefficient, $\left(\frac{\text{Thrust}}{qS}\right)$

F_Y lateral force, lb

M_X rolling moment, ft-lb

M_Y pitching moment, ft-lb

M_Z yawing moment, ft-lb

T thrust of ducts (including forces on outside of duct), lb

WM	windmilling propellers
S	reference area = 6.24 ft^2
c	reference chord = 1.50 ft
b	reference span = 8.32 ft
i_w	incidence of wing panels relative to fuselage centerline, deg
i_D	incidence of duct thrust axis relative to fuselage centerline (refers to all ducts unless used with subscript), deg

Subscripts F and R refer to front and rear duct, respectively.

Model

The model used in the investigation consisted of a boxy cargo-aircraft-type body on which the ducted propellers could be mounted in four arrangements as indicated in figures 1 and 2. A list of pertinent dimensional characteristics of the model is given in table I. The rear ducts could be mounted in either an inboard or outboard location high on the fuselage, and the front ducts could be mounted in either a high or low inboard location. The model was provided with two different types of vertical tails as indicated in figure 1 - a single centerline tail, or twin tails mounted on the ducts. The total area of the twin tails was the same as the area of the single tail. The model had fixed-pitch propellers, and all of the propellers were set at the same pitch. Changes in thrust were accomplished by changing the propeller rotational speed. The propellers were driven by separate electric motors in each duct; and the front and rear pairs of ducts were mounted to the body on strain-gage balances which permitted independent measurement of the thrust and normal force of the front and rear duct-propeller assemblies. The entire model, including ducts, was mounted on a third internal strain-gage balance which measured the total forces and moments on the model.

Tests

A series of tests was run in a 12-foot low-speed wind tunnel to study longitudinal stability in the cruise condition (duct incidence 0°). In these tests the size of the wing was varied for the configurations with the rear ducts inboard and the size of the vane in the front duct was varied for the configurations with the rear ducts outboard. The purpose of these tests was to select configurations which would give a reasonable amount of static longitudinal stability in the cruise condition for further tests in the transition condition. The configurations selected as a result of these tests are those shown in figures 1 and 2. The tests were made for a windmilling power condition and for a power-on condition $\left(T_c' = 0.5\right)$ corresponding to a level-flight condition at a high lift coefficient (C_L about 2.0). There were two rather serious faults with the data from these tests. One was that the gaps between the ducts, the body, and the wings were not sealed. The other was that because of the weight of the model the drag balance was not sufficiently sensitive to provide reliable drag data for the cruise conditions. Some data from these early tests are used in this paper however, because they are the only data available to show the effects of power on longitudinal stability in the normal-flight condition.

In another series of tests to study the drag of the model in the normal-flight condition, the model was lightened by removing the entire center body of the ducts (motors, propellers, and fairings) so that a more sensitive balance could be used, and the gaps between the body, ducts, and wings were sealed. These tests were, of course, made only for the power-off condition, and they were also made in the 12-foot low-speed tunnel.

A third series of tests to study the longitudinal stability and control problem in the transition range of flight was made in the 17-foot test section of the Langley 7- by 10-foot tunnel for configuration OB-HI. These tests were made for a range of duct incidence from 0° to 90° and included tests with different incidence on the front and rear ducts and with different thrust on the front and rear ducts. In these tests the incidence of the rear wing panel was always set at 0° relative to the fuselage axis.

A fourth series of tests was conducted in the Langley full-scale tunnel on configuration IB-LO to study both the longitudinal- and lateral-stability characteristics of the model in the transition range.

Results and Discussion

Normal Flight

Longitudinal stability.- The longitudinal-stability characteristics of the model in the normal forward flight range are illustrated by the curves of pitching moment versus lift coefficient in figures 3 and 4. These two figures show the stability curves for the four configurations, for three angles of incidence of the front ducts, and for two power conditions (windmilling propellers, and $T_c' = 0.5$). In all cases in which the model was stable, the curve is shown for the angle of incidence of the rear wing panel (not including the rear ducts or vanes behind the ducts) required for trim at a lift coefficient of 1.0, which corresponds to a cruise condition near maximum L/D. These data were taken from tests in which the gaps between the body, ducts, and wing panels were not sealed. Other power-off tests with the gaps sealed, however, showed that sealing the gaps caused only a small increase in stability $\left(\frac{dC_m}{dC_L}\right.$ about 0.03 more negative$\left.\right)$.

Three main points can be made from the data of figure 3 for the configurations having the rear duct in the inboard location. First, the stability characteristics seem reasonable except for the $i_{D_F} = 5^\circ$ condition which has a marked pitch-up tendency. This pitch-up is evidently the result of early stall of the rear wing panels at the high angles of incidence required for trim with the front duct at 5° incidence. This stall may well be aggravated by upwash caused by the tip vortices from the front ducts. The second point is that there is no consistent effect of power on stability, and that the effect of power is not extremely large. And, the third point is that there is little change in trim with power at $i_{D_F} = 0^\circ$ for the IB-LO configuration.

Three main points are also brought out by the data of figure 4 for the configurations having the rear duct in the outboard location. First, comparison of these data with those of figure 3 shows that these configurations are more prone to pitch-up than the inboard-rear-duct configurations. All of the configurations except the OB-HI configuration with $i_{D_F} = 0^\circ$ show a pronounced pitch-up. The second point is that power has a major effect on stability in relieving the pitch-up. This effect of power evidently results from the fact that the increased downwash from the front duct caused by power reduces the angle of attack of the rear wing panel and delays its stall. And, the third point is that power has little effect on trim for the $i_{D_F} = 0^\circ$ condition.

Lateral stability.- The lateral-stability characteristics of the model in the cruise condition are shown in figure 5 for configuration IB-LO. This is the only configuration for which lateral data have been obtained. The tests were made for the power-on condition with $C_D = 0$.

The data show that the model had only about neutral directional stability with the particular tails tested. The tail effectiveness was about constant over the angle-of-attack range, however, so it would seem that the directional stability could have been made adequate by the use of slightly larger vertical tails. It is also interesting to note that the directional stability was somewhat better with the simpler single vertical tail than with the twin vertical tails.

The data of figure 5 also show that the values of C_{Y_β} for the model were very high. Actually they are about one-half as high as the slope of the lift curve C_{L_α} which was about 0.15, and if some allowance is made for the fact that a larger vertical tail is required for adequate directional stability, the value of C_{Y_β} would be an even larger percentage of C_{L_α}. These high values of C_{Y_β} would seem to mean that an airplane of this type would be unusually rough riding because of its high response to side gusts. For example, a standard 30-foot-per-second side gust would give a sidewise acceleration one-half as great as the normal acceleration caused by a standard 30-foot-per-second vertical gust, and sidewise accelerations would seem to be more objectionable than normal acceleration to the occupants of the airplane.

The effective dihedral of the model, as indicated by the parameter C_{l_β} in figure 5, seems fairly normal when allowance is made for relatively small wing area on which C_l is based. A word of caution is in order in connection with these C_{l_β} values, however. That is that the values were read from some very nonlinear curves of C_l versus β so that they are at best only a rough indication of the dihedral effect.

Lift.- Lift curves for the rear-duct-outboard and rear-duct-inboard configurations are shown in figure 6. Only two curves are shown since the curves are almost identical for configurations with the front ducts high or low. These curves were taken from the power-off tests with the propellers and duct center bodies removed and with the gaps between the body, ducts, and wing panels sealed.

The lift curves are quite nonlinear, but measurements of the lift-curve slope (either the slope at zero lift or the average slope) shows that lift-curve slope C_{L_α} is about 20 percent higher for the outboard-duct configuration than for the inboard-duct configuration. This is a considerably greater difference than would be expected on the basis of the 2-percent greater lifting area and 4-percent greater span of the rear-duct-outboard configurations. The difference in lift-curve slope therefore probably results partly from the fact that the ducts on the tip of the rear wing give it a higher effective aspect ratio and partly from the fact that the downwash from the front ducts reduces the lift-curve slope of the smaller lifting surface of the rear wing panel rather than the larger biplane-type lifting surface of the rear ducts.

Drag.- The drag characteristics of the model are shown in figure 7 for configurations IB-LO and OB-HI. Drag data are not shown for the other two configurations since their drag curves were so irregular as to be of little use in analysis. The drag curves shown in figure 7 were taken from the power-off tests with the propellers and duct center bodies removed and with the gaps between the body, ducts, and wing panels sealed. These drag curves are for the trimmed condition ($C_m = 0$) with the model trimmed with the most favorable combination of incidence of the front ducts and incidence of the rear wing panel.

The data of figure 7 show that the induced drag of the OB-HI configuration is considerably lower than that of the IB-LO configuration even

though the wing span and total lifting area of the two configurations are very nearly the same. In fact, the span efficiency factor e of the rear-duct-outboard configuration calculated from these curves is 0.76 while that for the rear-duct-inboard configuration is 0.65. Or, in other terms, the ratio of effective span to actual span of the OB-HI configuration is 8 percent greater than that of the IB-LO configuration. This fact in itself does not necessarily indicate a superiority of one configuration over the other. The induced drag of the IB-LO configuration could presumably be made as low as that of the OB-HI configuration by increasing its wing span and taking other appropriate steps to adjust the longitudinal stability. The above values of span efficiency factor may seem low compared with those of conventional aircraft, but the value of 0.76 is actually fairly representative of the value of e of a conventional multiengine airplane model of the same low scale.

Transition

As the airspeed approaches zero in the transition range of flight, conventional nondimensional aerodynamic coefficients approach infinity. In this case it is felt that the analyst will have a readier understanding of the results in dimensional form than in the form of conventional aerodynamic coefficients. For this reason the data for the transition range of flight are presented in dimensional form for the model at a lift of 100 pounds.

Longitudinal stability and trim.- The results of tests to determine the basic longitudinal-stability and trim characteristics of the OB-HI and IB-LO configurations in the transition range are shown in figure 8. In these tests the blade angle and rotational speed of the front and rear propellers were the same and the incidence of the front and rear ducts was the same. The incidence of the rear wing panels was 0° relative to the fuselage axis for the OB-HI configuration and -15° relative to the rear duct thrust axis for the IB-LO configuration.

The data of figure 8 show that the OB-HI configuration had large nose-up pitching moments which reached a maximum at 60° or 70° incidence and that the moments for the IB-LO configuration were much lower. The magnitude of the moment at the peak for the OB-HI configuration corresponds to a rearward shift of the center of pressure of 0.60 propeller diameter.

The data of figure 8 also show that the model had a very low degree of static longitudinal instability over the transition range. Some idea of the significance of the magnitude of the values of the M_α shown can be gained by comparing them with those of other VTOL aircraft configurations that have been flown. For example, the maximum unstable value shown ($M_\alpha = 2$) is about 1/20 that of a comparable model of a tilt-wing VTOL airplane that has been flown successfully with no complaint about the instability.

The results of tests to determine the effectiveness of differential duct incidence and differential thrust in trimming out the nose-up pitching moments in the transition range for the OB-HI configuration are presented in figure 9. These data show that differential thrust (higher thrust on the rear ducts than on the front ducts) was very effective in reducing the nose-up pitching moments at high-duct-incidence conditions, but that it was relatively ineffective at low-duct-incidence conditions. The data also show that the use of differential duct incidence (lower incidence on the front ducts than on the rear ones) was very effective in reducing the nose-up pitching moment at low-duct-incidence conditions but was relatively ineffective at high-duct-incidence conditions. These results suggest that the model could be trimmed readily with appropriate combinations of differential duct angle and differential thrust. It therefore seems apparent that the much smaller pitching moments of the IB-LO configuration could be trimmed quite easily, but no test data are available to substantiate this reasoning.

The data of figure 10 show the effect of acceleration and deceleration on longitudinal stability and trim for the IB-LO configuration. This is the only configuration for which such data are available at the present time. In these tests the incidence of the rear wing panel was 0° relative to the fuselage axis throughout the transition range. The 1/4g acceleration condition shown in the figure can also be considered to represent a 14° climb and the 1/4g deceleration condition corresponds to a 14° descent.

The data of figure 10 show that there is essentially no change in the maximum nose-up pitching moment that must be trimmed out in the transition range. In this respect this configuration is different from many other VTOL aircraft configurations in which the nose-up pitching moment is much greater for the deceleration or descent condition than for the zero acceleration level-flight condition.

Lateral stability.- The lateral-stability characteristics of the model are presented in figure 11 for the IB-LO configuration. This is the only configuration for which lateral data have been obtained in the transition range. In these tests the front and rear ducts were set at the same incidence and the power was that required for zero drag at zero fuselage angle and zero sideslip. The data show that the model was directionally stable and had a positive dihedral effect throughout the transition range with the single vertical tail.

Summary of Results

The principal results of the investigation may be summarized as follows:

1. For the cruise condition, acceptable longitudinal stability could be obtained with either rear-duct-inboard or rear-duct-outboard configurations.

2. In the cruise condition, the slope of the lift curve was higher and the induced drag was lower for the rear-duct-outboard configuration than for the rear-duct-inboard configuration for approximately equal wing area and span.

3. In the transition condition the rear-duct-outboard configuration experienced large nose-up pitching moments. It was possible, however, to trim out these pitching moments with appropriate combinations of differential duct incidence and differential thrust on the front and rear ducts.

4. Satisfactory directional stability could be obtained in both the cruise and transition conditions for the rear-duct-inboard configuration - the only one for which lateral data were obtained.

5. The lateral tests also showed that in the cruise condition the model had a variation of lateral force with angle of sideslip that was abnormally high - about one-half as great as the slope of the lift curve.

TABLE I

DIMENSIONS OF MODEL

(All dimensions in inches)

Body:	
Maximum height	15.4
Maximum width	15.4
Length	86
Distance of forward duct pivot aft of nose	11
Distance between duct pivots	53.2
Distance of rear duct pivot below top of fuselage	2.4
Distance of front duct pivot below top of fuselage	
High duct location	2.4
Low duct location	13.0

	Rear duct inboard	Rear duct outboard
Wing:		
Span	75.6	78.6
Chord	12	12

	Center	Twin (each)
Vertical tail:		
Area	284	142
Height (from top of fuselage)	19.4	13.7
Root chord	19.4	13.7
Tip chord	9.8	6.9

Ducts:	
Outside diameter	17.25
Inside diameter	14.0
Exit diameter	15.96
Length	9.0
Pivot point, percent duct chord	50
Vane span	15.96
Vane chord	3.4
Propeller:	
Diameter	13.75

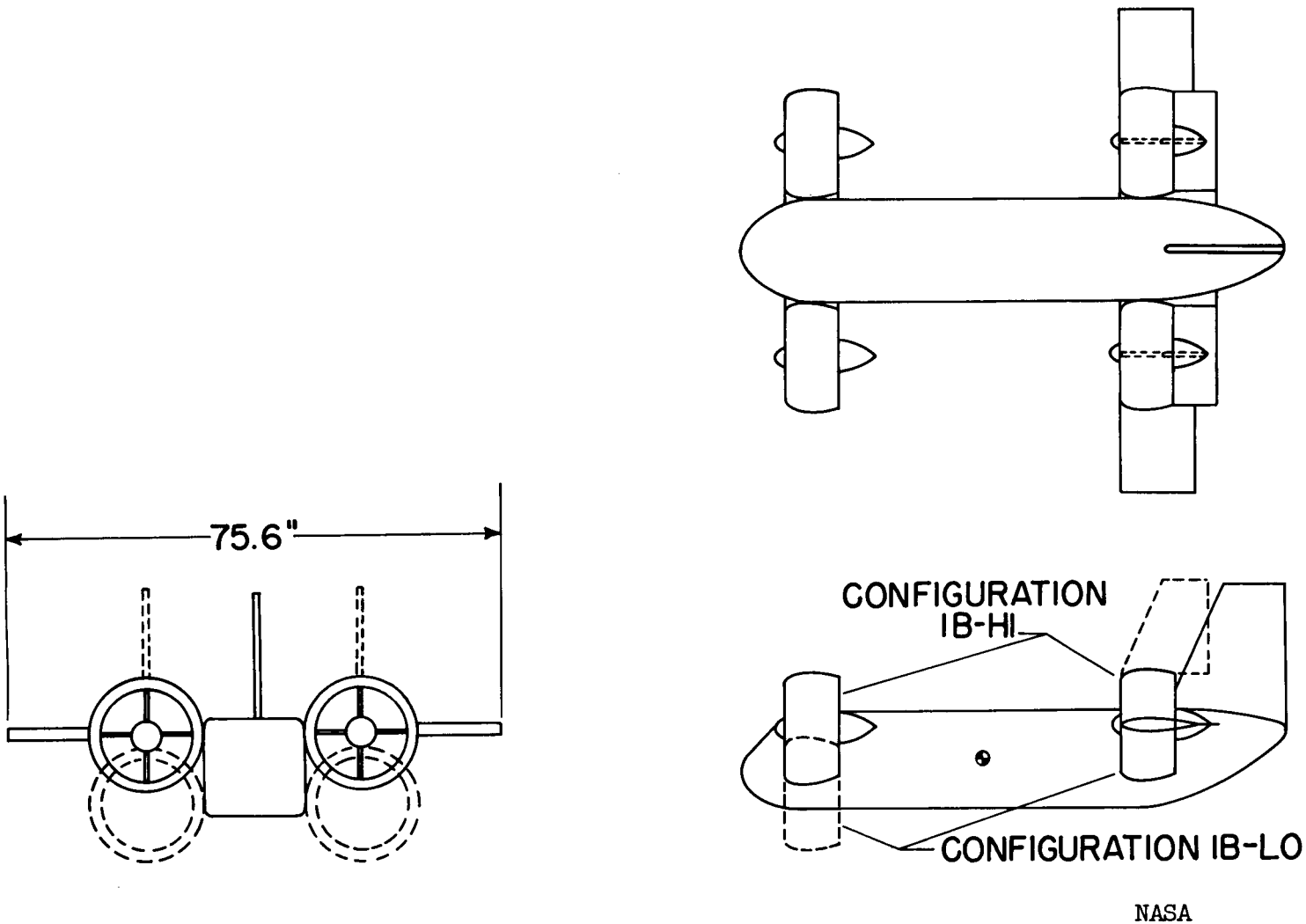

Figure 1.- Model with rear ducts inboard.

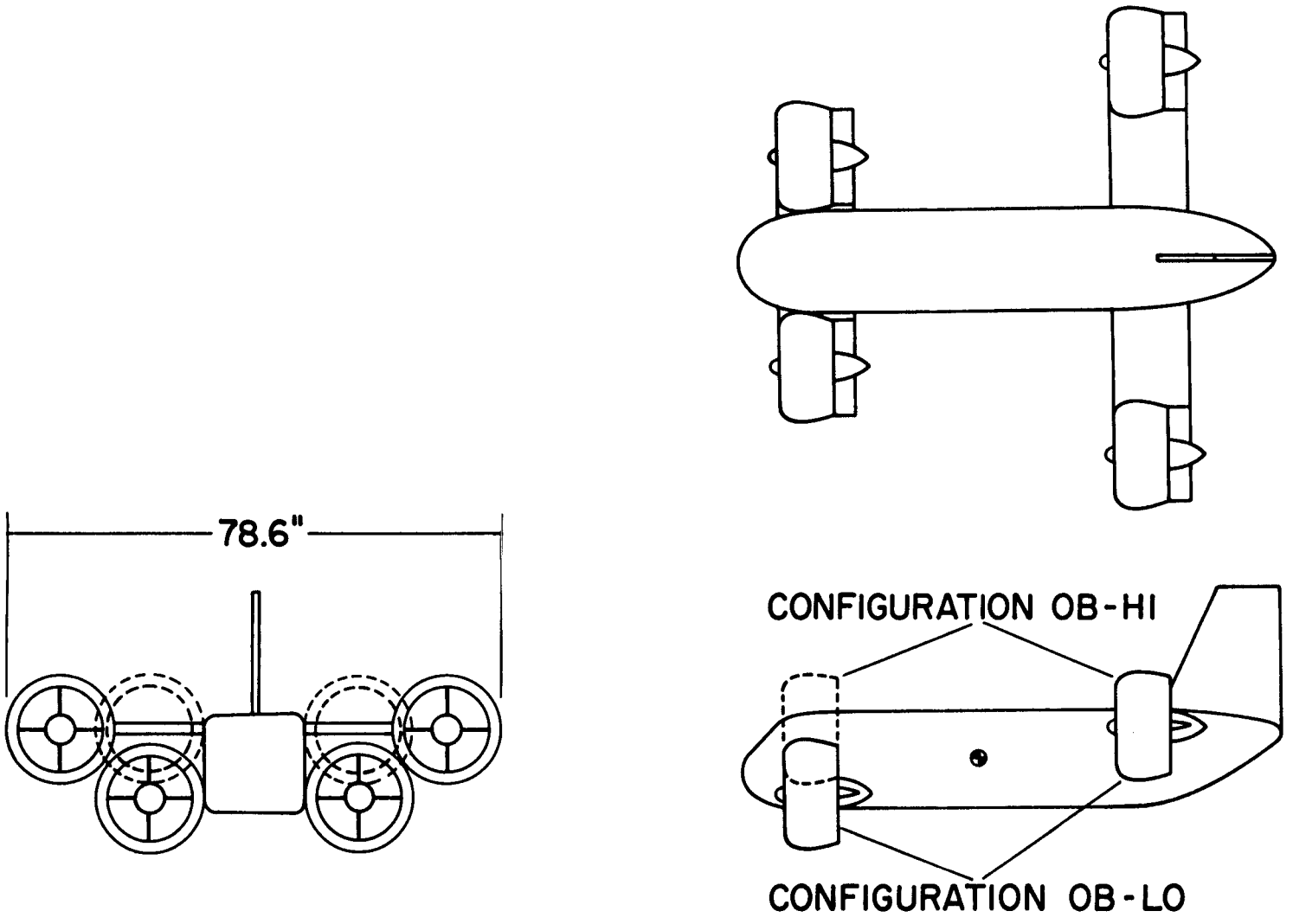

Figure 2.- Model with rear ducts outboard.

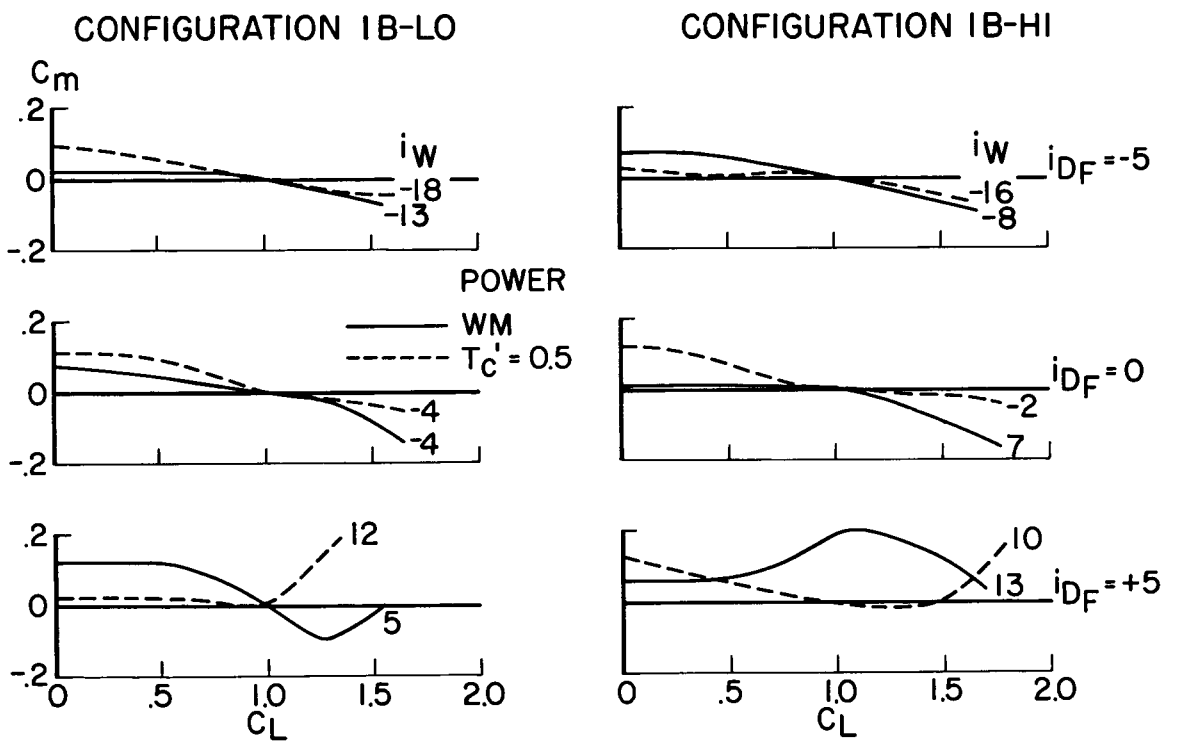

NASA

Figure 3.- Longitudinal stability in cruise, rear ducts inboard.

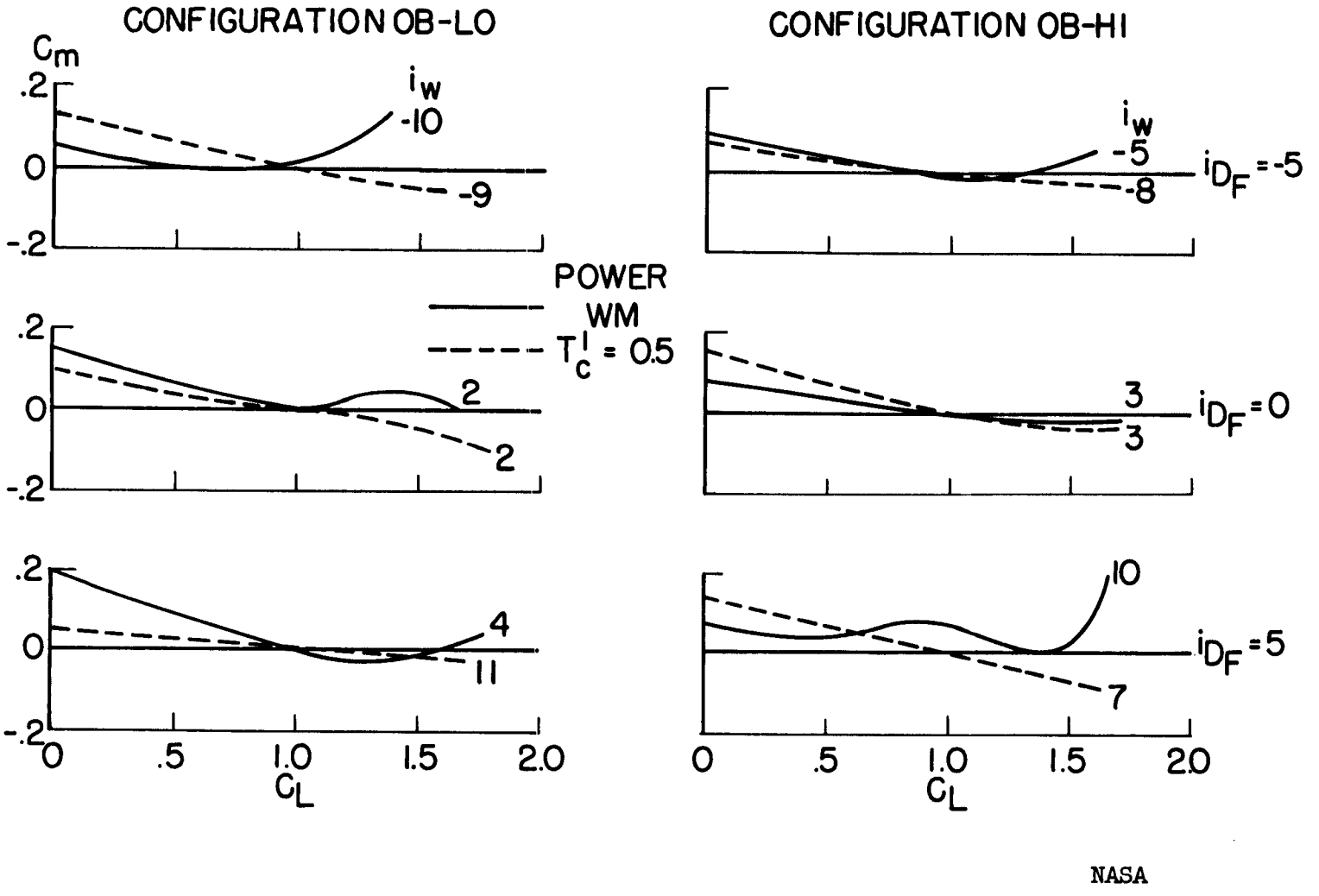

Figure 4.- Longitudinal stability in cruise, rear ducts outboard.

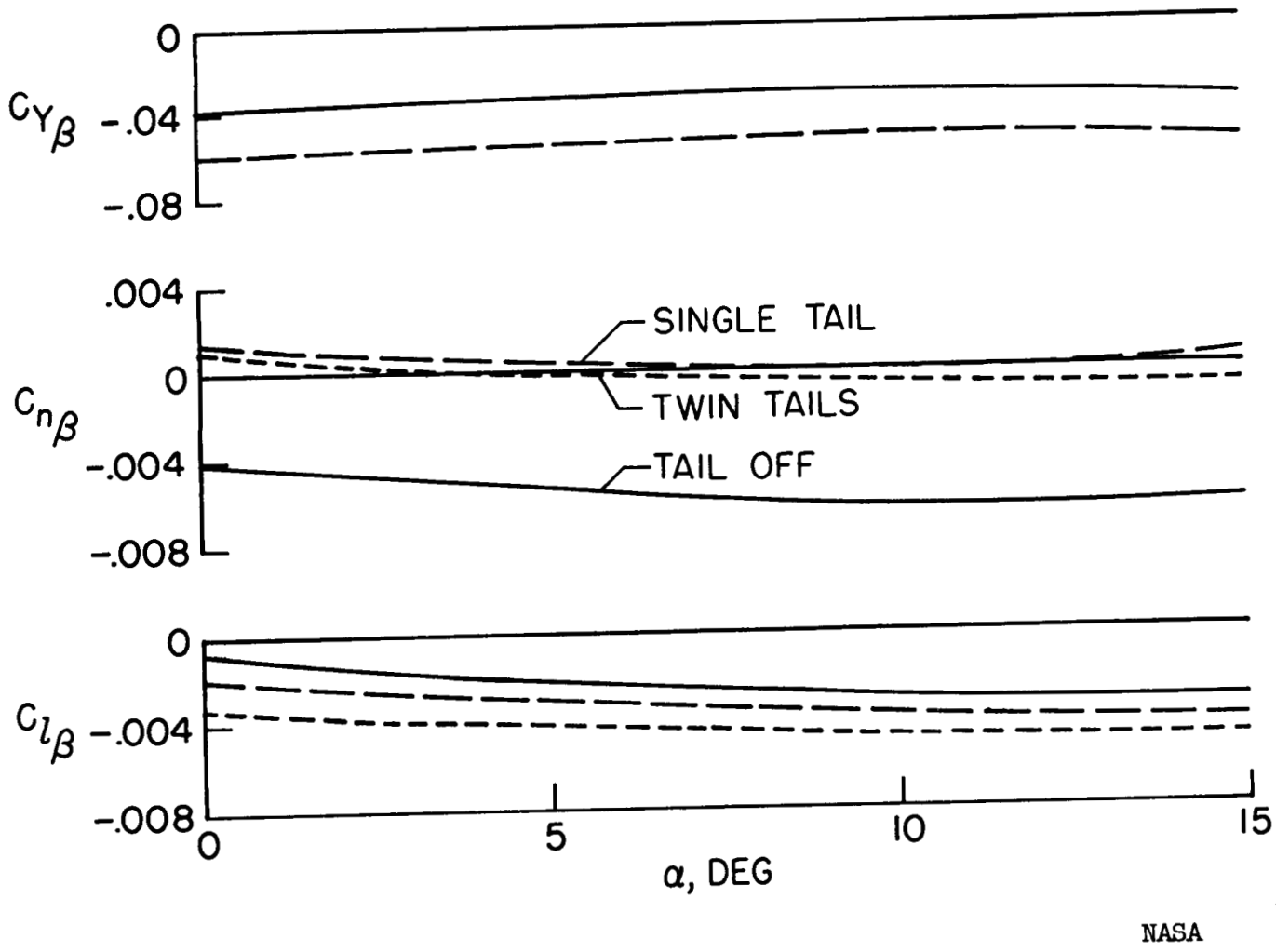

Figure 5.- Lateral stability in cruise.

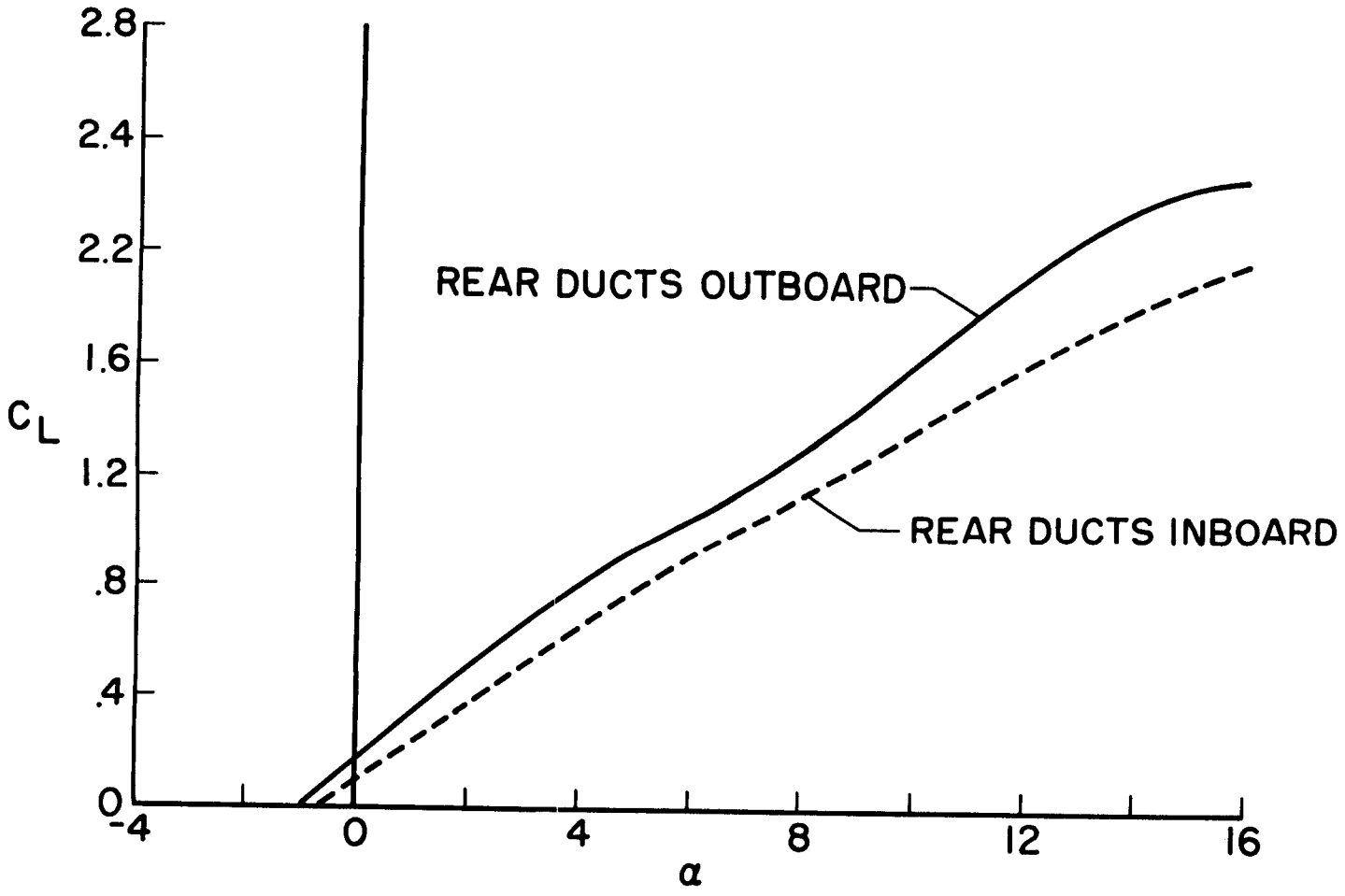

Figure 6.- Lift characteristics in cruise.

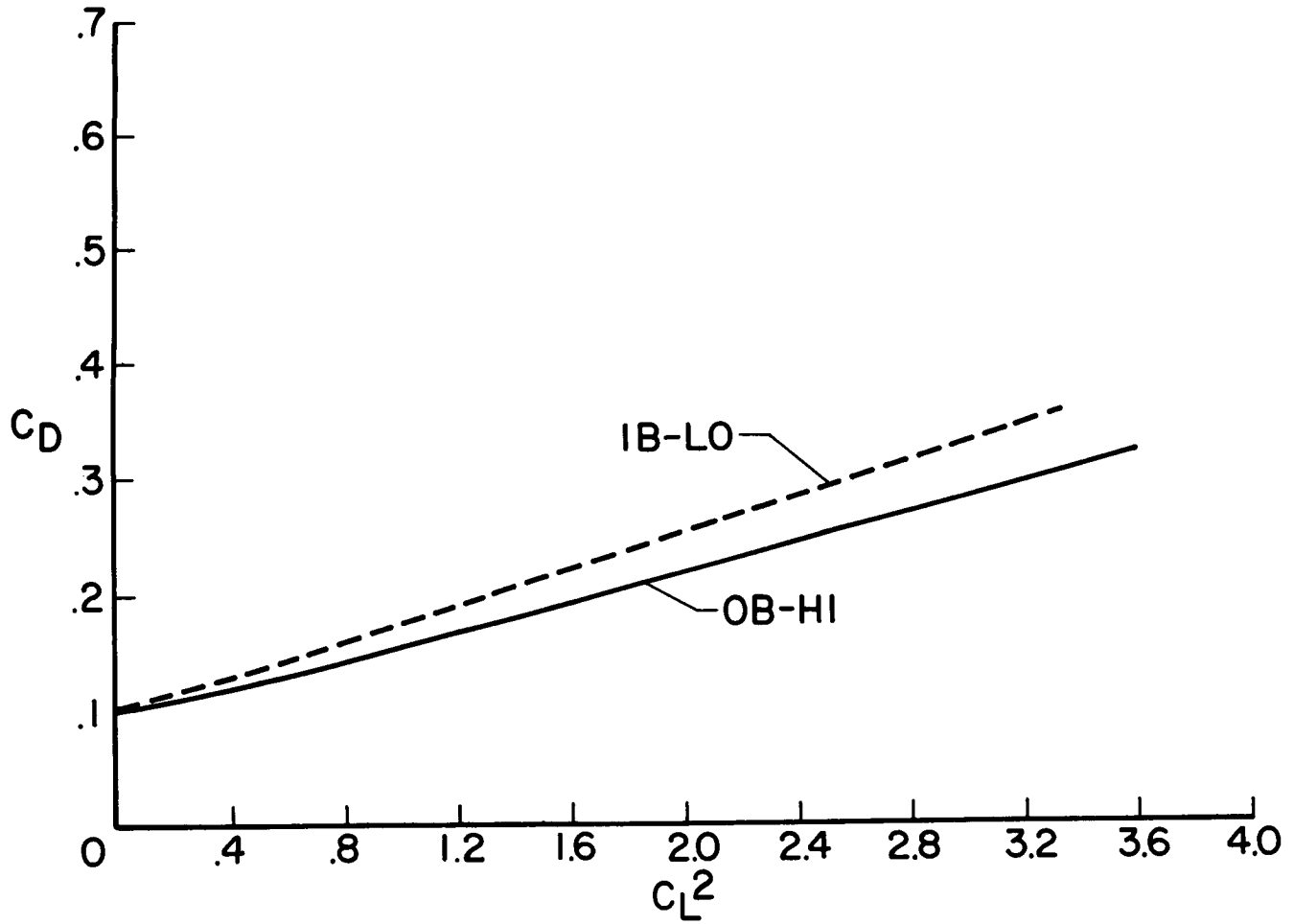

Figure 7.- Drag characteristics in cruise.

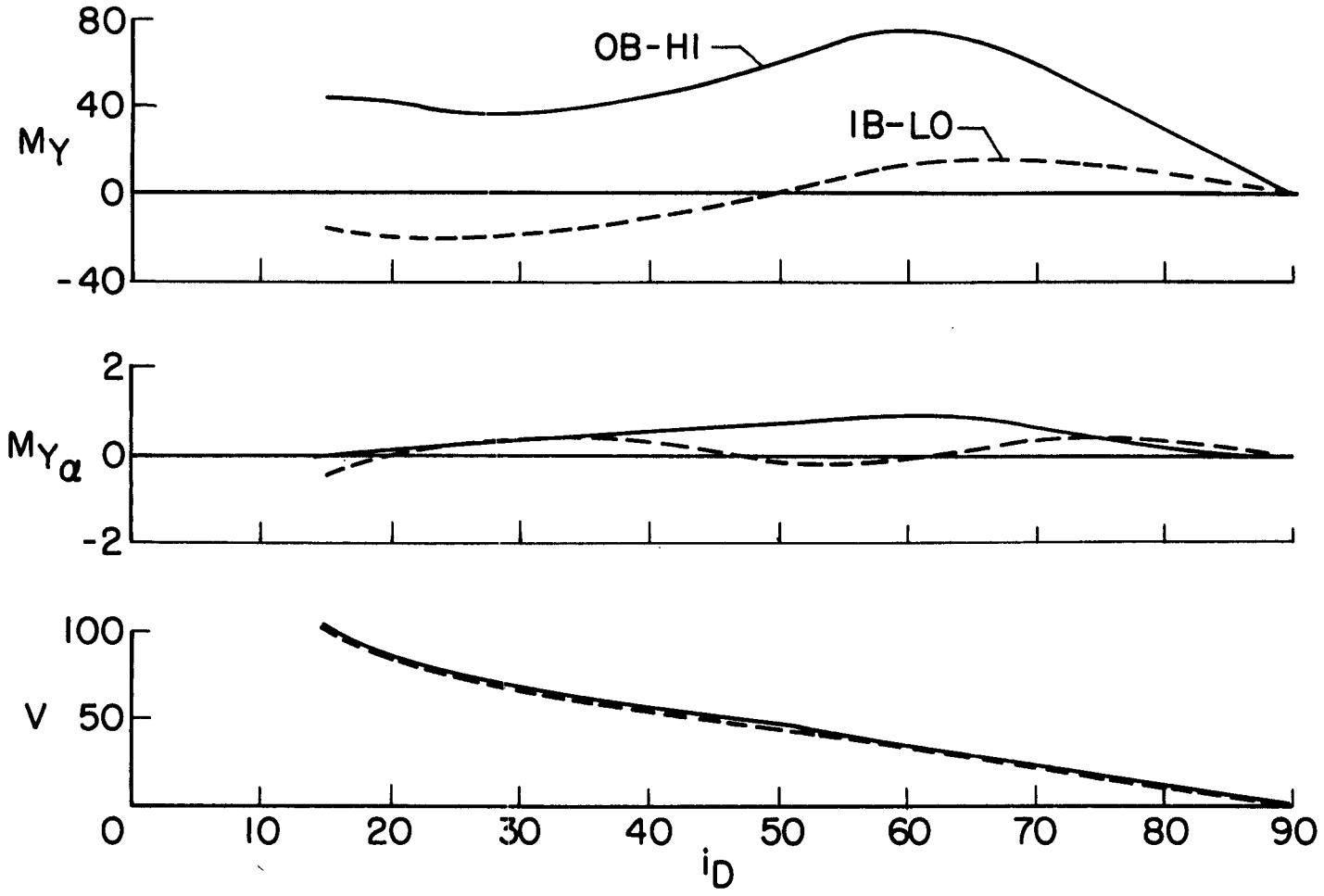

Figure 8.- Longitudinal stability and trim in transition.
$RPM_F = RPM_R$; $\alpha = 0^\circ$; Drag = 0.

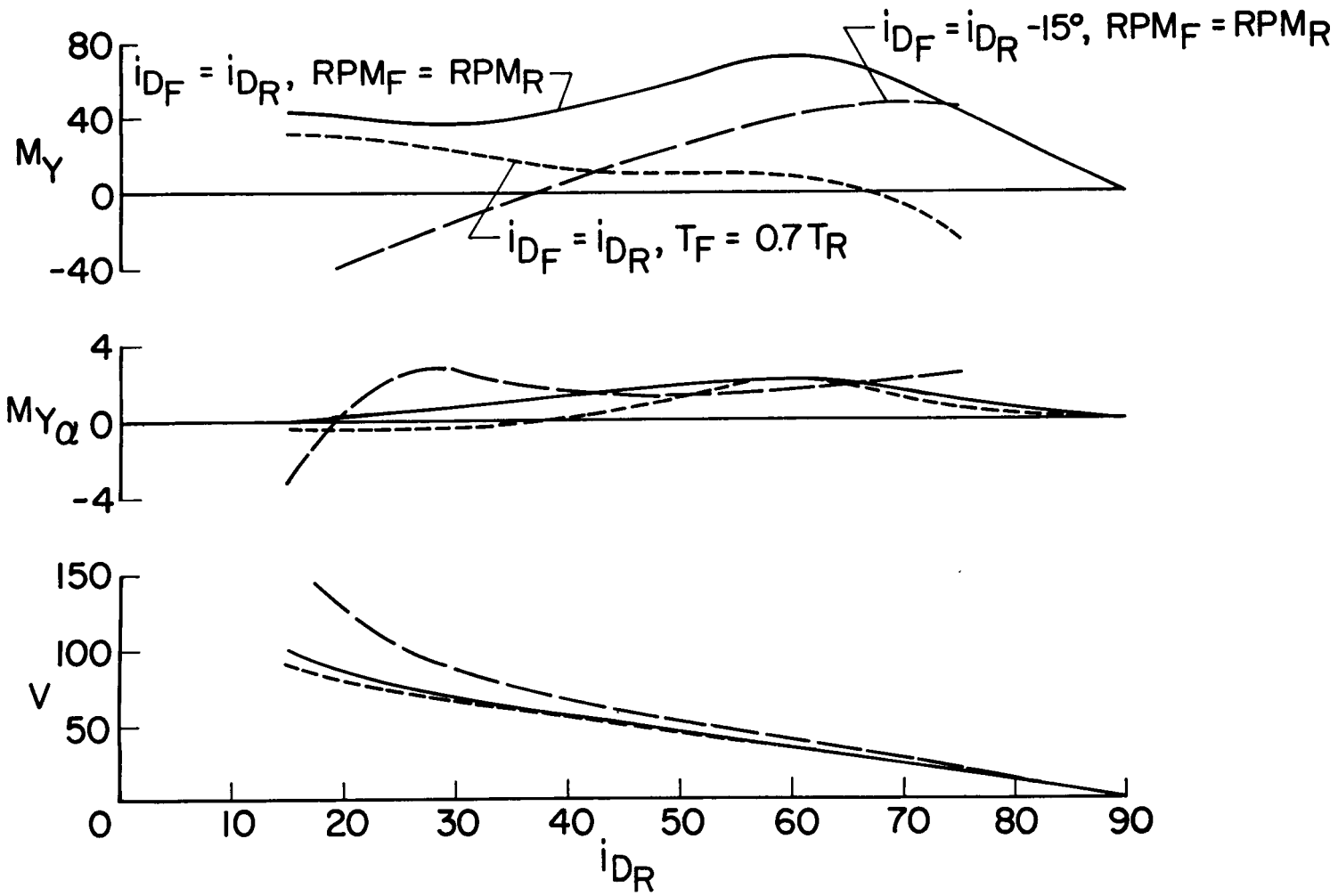

Figure 9.- Effect of differential duct incidence and thrust.
Configuration OB-HI; $\alpha = 0^\circ$; Drag = 0.

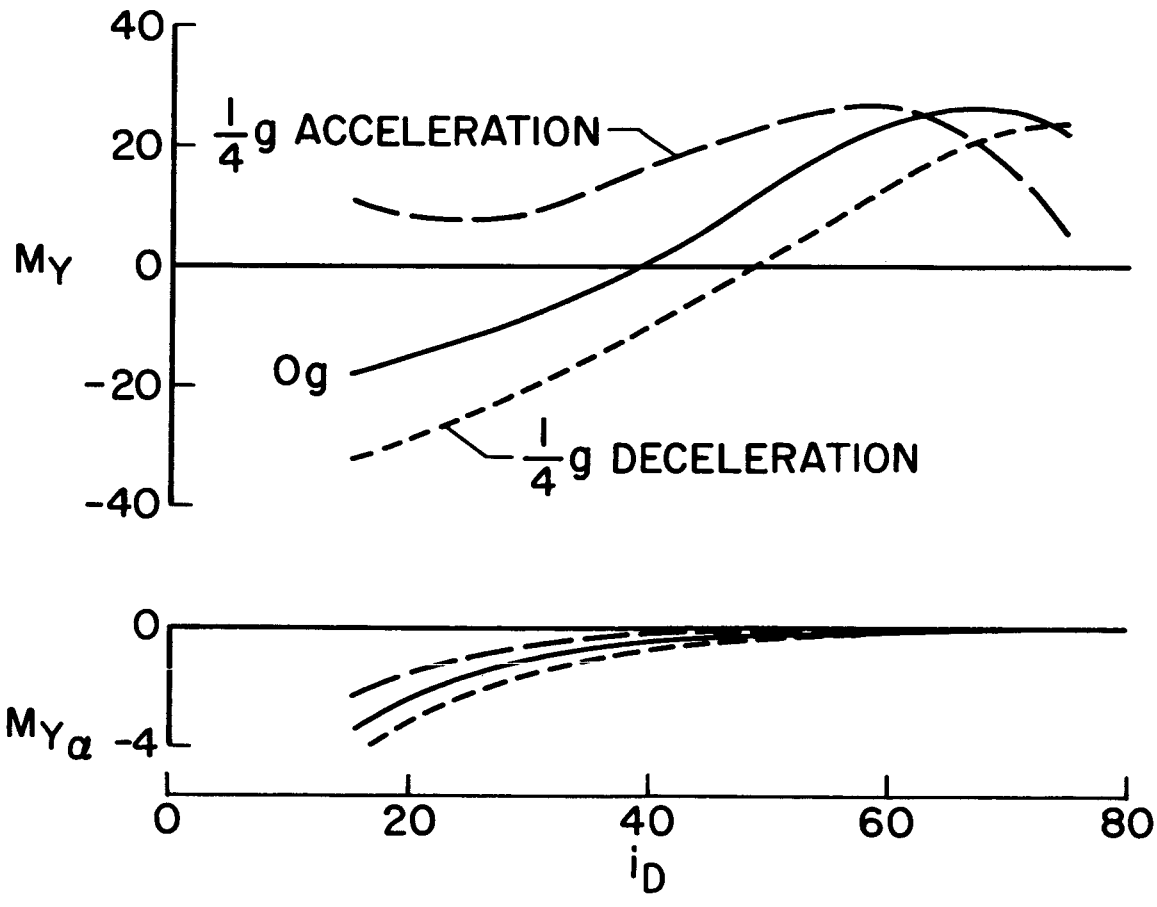

Figure 10.- Effect of longitudinal acceleration.
Configuration IB-LO.

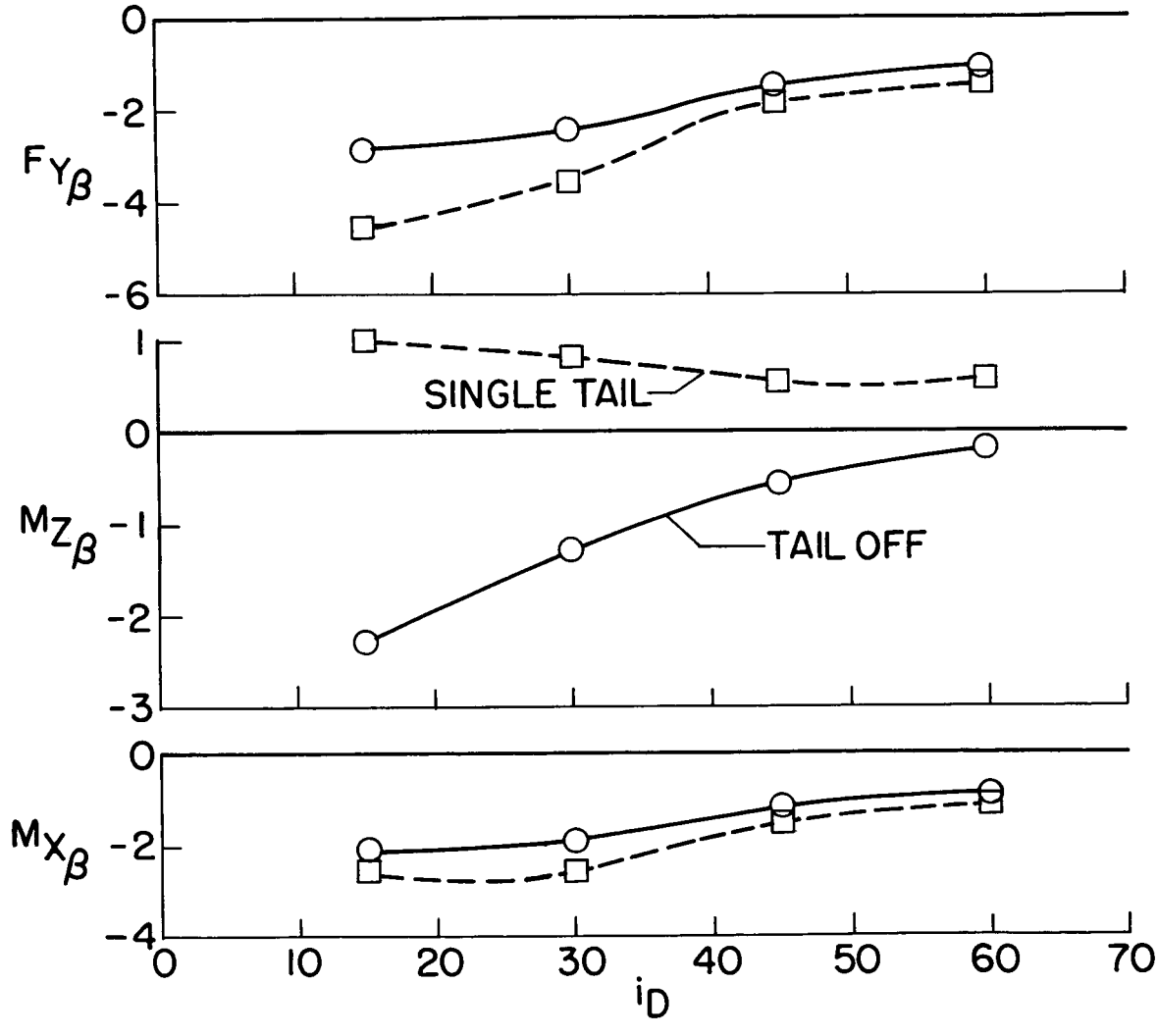

NASA

Figure 11.- Lateral stability in transition. Configuration IB-LO; $i_{D_F} = i_{D_R}$.